Journal of Medicinal Chemistry

Article

pubs.acs.org/jmc

Selenorhodamine Photosensitizers for Photodynamic Therapy of P-Glycoprotein-Expressing Cancer Cells

Jacqueline E. Hill,[†] Michelle K. Linder,[†] Kellie S. Davies,[†] Geri A. Sawada,[‡] Janet Morgan,[§,⊥] Tymish Y. Ohulchanskyy,[∥] and Michael R. Detty*[,†,∥]

[†]Department of Chemistry, University at Buffalo, The State University of New York, Buffalo, New York 14260-3000, United States

[‡]Drug Disposition, Eli Lilly and Company, Indianapolis, Indiana 46285, United States

[§]Department of Dermatology, Roswell Park Cancer Institute, Elm and Carlton Streets, Buffalo, New York 14263, United States

[∥]Institute for Lasers, Photonics and Biophotonics, Department of Chemistry, University at Buffalo, The State University of New York, Buffalo, New York 14260, United States

Supporting Information

ABSTRACT: We examined a series of selenorhodamines with amide and thioamide functionality at the 5-position of a 9-(2-thienyl) substituent on the selenorhodamine core for their potential as photosensitizers for photodynamic therapy (PDT) in P-glycoprotein (P-gp) expressing cells. These compounds were examined for their photophysical properties (absorption, fluorescence, and ability to generate singlet oxygen), for their uptake into Colo-26 cells in the absence or presence of verapamil, for their dark and phototoxicity toward Colo-26 cells, for their rates of transport in monolayers of multidrug-resistant, P-gp-overexpressing MDCKII-MDR1 cells, and for their colocalization with mitochondrial specific agents in Colo-26 cells. Thioamide derivatives **16b** and **18b** were more effective photosensitizers than amide derivatives **15b** and **17b**. Selenorhodamine thioamides **16b** and **18b** were useful in a combination therapy to treat Colo-26 cells in vitro: a synergistic therapeutic effect was observed when Colo-26 cells were exposed to PDT and treatment with the cancer drug doxorubicin.

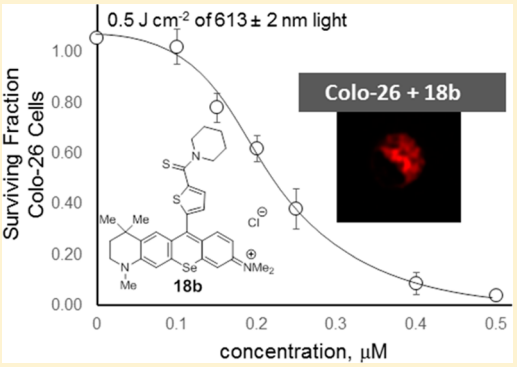

INTRODUCTION

The treatment of cancer cells expressing P-glycoprotein (P-gp, also known as MDR1 or ABCB1) or other ABC transporters is often limited by the ability of the chemotherapeutic agent to penetrate the cellular membrane in the presence of the ABC transporter.[1] P-gp expression and associated drug resistance can be quite rapid, with *mdr* gene expression commencing within an hour of treatment.[3] Effective clinical intervention with multidrug-resistant (MDR) cancer will require design of mechanism-based inhibitors of P-gp and other multidrug-binding proteins. Currently, there are no approved reversal agents for use in the clinic.[4−6]

As a class, the rhodamines are transported rapidly by P-gp with tetramethylrosamine [**1** (E = O), Chart 1] being transported roughly 5- to 10-fold faster than either rhodamine 123 (**2**) or rhodamine 6G (**3**) in isolated P-gp.[7−9] In non-drug-resistant cancer, rhodamines have found therapeutic applications as anticancer agents. As delocalized lipophilic cations (DLCs), rhodamines are concentrated in the mitochondria of cancer cells because of increased mitochondrial membrane potential in the transformed cells.[10,11] Rhodamine 123 (**2**) has also been used to treat cancers in vitro[12] and in vivo.[13] Other DLCs such as the thiopyrylium dye **4** are also cytotoxic to cancer cells in vitro and have antitumor activity in vivo.[14]

Photodynamic therapy (PDT) is a treatment modality for a variety of cancers including cancers of the lung, gastrointestinal tract, the head and neck region, bladder, prostate, and nonmelanoma skin cancer.[15] In PDT, irradiation of a cancer-targeted, light absorbing molecule (a photosensitizer) leads to phototoxicity beyond any observed dark toxicity toward the cancer.[15] While in principle, the rhodamines and **4**-like dye molecules have the potential to be photosensitizers for PDT of cancer,[15] irradiation of cells or tumors treated with **2** or **4** gives no increase in toxicity in vitro[11,14] or in vivo.[13,14] Furthermore, one might ask whether rhodamine derivatives, which are excellent transport substrates for P-gp, would function as effective photosensitizers in cancers showing drug resistance.

Among the attributes of an ideal photosensitizer are (1) strong, high extinction coefficient absorbance in the 600−800 nm window, where tissue penetration of light is at a maximum and where wavelengths of light are still energetic enough to produce $^1O_2$, (2) a high quantum yield for the photochemical event [production of $^1O_2$ or other reactive oxygen species (ROS)], and (3) targeting of the desired tissue or cellular/subcellular site.[15] While rhodamines selectively target the

Received: August 16, 2014
Published: September 24, 2014

   dx.doi.org/10.1021/jm501259v | J. Med. Chem. 2014, 57, 8622−8634

Chart 1. Structures of the Chalcogenorosamines [1 (E = O, S, Se)], Rhodamine 123 (1), Rhodamine 6G (2), Thiopyrylium 4, Rhodamines 5, and Julolidylrosamines 6 (E = S, Se)

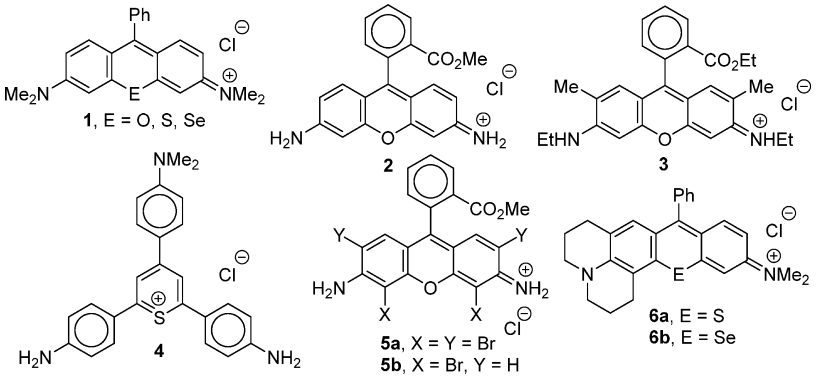

Chart 2. Structures of Thiorhodamines 7a–18a and Selenorhodamines 15b–18b

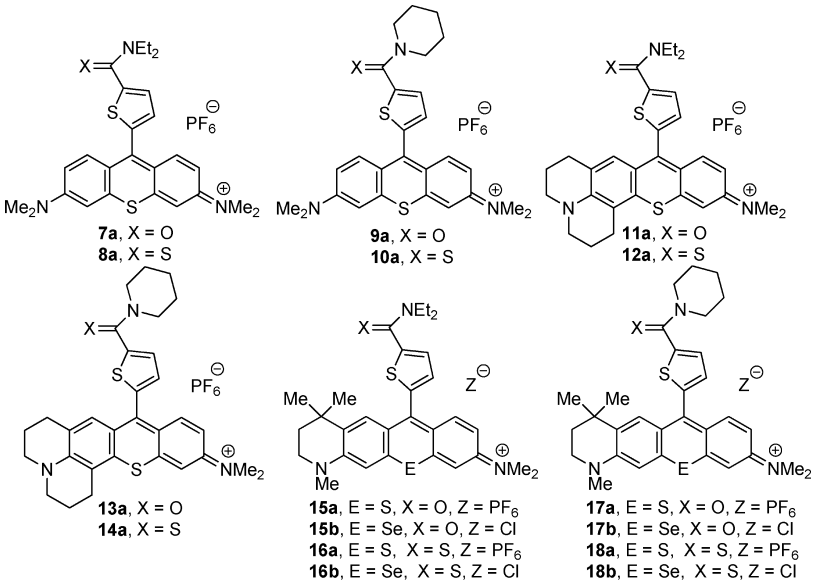

mitochondria of transformed cells, they are poor photosensitizers, absorbing wavelengths of light too short for effective penetration of tissue and producing $^1O_2$ and other ROS inefficiently.[16,17]

Rhodamines brominated on the xanthylium core have increased quantum yields for the generation of $^1O_2$ [$\Phi(^1O_2)$] due to heavy atom effects from bromine.[16] Tetrabromo derivative **5a**[18] and dibromo derivative **5b**[19] (Chart 1) still target mitochondria and are phototoxic to transformed cells, but wavelengths of absorption are unchanged relative to **2**. Dibromorhodamine **5b** has been evaluated in several clinical trials.[19] Replacing the oxygen atom of the xanthylium core of **1** with the heavier chalcogen atoms S or Se (Chart 1) gives derivatives with longer wavelengths of absorption and increased values of $\Phi(^1O_2)$.[17] These derivatives are phototoxic and target the mitochondria of cancer cells, but both the thio- [**1** (E = S)] and selenorosamine [**1** (E = Se)] have values of λ_{max} < 600 nm,[17,20] which will limit their utility in vivo.

When examining the role of rhodamine-derived photosensitizers in the PDT of MDR cells, one must reconcile the rapid transport of the rhodamines by P-gp out of the cell with the mitochondrial specificity of the rhodamines. The transport of **2** was used to define substrates and antagonists for P-gp in the NCI 60 set of cells with the NCI Drug Screen Database of compounds.[21,22] The rhodamine binding site (the "R" site) in P-gp was first suggested by Shapiro and Ling to define that rhodamines, in general, are substrates for P-gp.[23,24] With the assumption that the rhodamines have a common locus for binding, we examined several discrete libraries of rhodamine/rosamine compounds for their ability to stimulate ATPase activity leading to active transport.[25,26] These studies indicated a greater than a 1000-fold variation in ATPase activities with small structural changes within the rhodamines/rosamines.[25,26]

With respect to rates of rhodamine transport, single atom changes can also give large differences in transport rates in a P-gp-expressing monolayer of cells in both absorptive transport (apical to basolateral transport, P_{AB}) and secretory transport (basolateral to apical transport, P_{BA}). The ratio of secretory to absorptive transport (P_{BA}/P_{AB}) is an excellent indicator of whether a compound is a substrate for P-gp transport. For chalcogenorosamines **1** (E = O, S) and the julolidylrosamine **6a** (Chart 1), values of P_{BA}/P_{AB} are large, in the range of 149–450.[27] Replacing the sulfur atom with a selenium atom in **6b** (Chart 1) gave a P_{BA}/P_{AB} of 15, which is at least an order of magnitude smaller.[27] Another single-atom change with tremendous impact on P_{BA} is the "amide/thioamide switch" in which amide derivatives **7a**, **9a**, **11a**, **13a**, **15a**, and **17a** (Chart 2) have values of P_{BA} that are 1.5- to 7-fold greater than

dx.doi.org/10.1021/jm501259v | J. Med. Chem. 2014, 57, 8622–8634

Scheme 1. Synthesis of Selenorhodamines 15b−18b

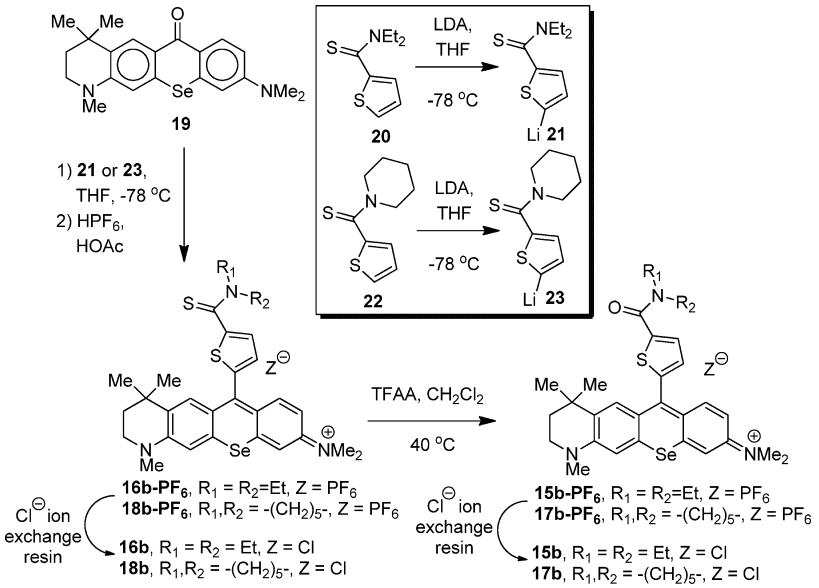

Table 1. Absorption Maxima (λ_{max}) and Molar Extinction Coefficients (ε) in CH_3OH, Fluorescence Emission Maxima (λ_{FL}) and Quantum Yields for Fluorescence (Φ_{FL}) in CH_3OH, Quantum Yields for the Generation of Singlet Oxygen [$\Phi(^1O_2)$] in CH_3OH, *n*-Octanol/Water Partition Coefficients (log *P*) for Thiorhodamines 15a−18a and Selenorhodamines 15b−18b[a]

compd	λ_{max}, nm	ε, M^{-1} cm^{-1}	λ_{FL}, nm	Φ_{FL}	$\Phi(^1O_2)$	log *P*
15a[b]	597	6.77×10^4	626	0.09 ± 0.01	<0.05	1.4
15b	609	7.18×10^4	636	0.009 ± 0.001	0.50 ± 0.03	2.26 ± 0.04
16a[b]	597	6.30×10^4	626	0.07 ± 0.01	<0.05	2.7
16b	608	9.78×10^4	635	0.008 ± 0.001	0.54 ± 0.03	2.41 ± 0.04
17a[b]	598	8.31×10^4	626	0.09 ± 0.01	<0.05	1.7
17b	609	8.73×10^4	634	0.009 ± 0.001	0.48 ± 0.03	2.23 ± 0.04
18a[b]	598	6.18×10^4	626	0.07 ± 0.01	<0.05	2.6
18b	608	8.11×10^4	634	0.008 ± 0.001	0.44 ± 0.03	1.61 ± 0.06

[a]Error limits are ±SD. [b]Values of λ_{max}, ε, and log *P* for **15a−18a** are taken from ref 28.

the corresponding thioamide derivatives **8a**, **10a**, **12a**, **14a**, **16a**, and **18a**, respectively (Chart 2).[28] Among these 12 examples, P_{BA} for amide **17a** ($P_{BA} = 230 \times 10^{-9}$ m s^{-1}) was 7-fold greater than P_{BA} for thioamide **18a** ($P_{BA} = 34 \times 10^{-9}$ m s^{-1}).[28]

The amide and thioamide derivatives of thiorhodamines **7a**−**18a** shown in Chart 2 were also micromolar inhibitors of P-gp. The tetrahydroquinoline derivatives **15a**−**18a** display the greatest ability to inhibit P-gp in whole cell studies based on values of IC_{50} for the enhancement of calcein AM (CAM) uptake into MDCKII-MDR1 transfected cells.[28]

The tetrahydroquinoline derivatives **15a**−**18a** have not been evaluated as photosensitizers for PDT. If these molecules were to generate ROS such as $^1O_2$ efficiently upon irradiation, then they should be effective photosensitizers toward P-gp-expressing cells, since their inhibitory effects toward P-gp transport would allow increased photosensitizer uptake and, presumably, greater efficacy in P-gp expressing cells. Incorporation of a heavy atom into **15a**−**18a** should give increased triplet yields and increased values of $\Phi(^1O_2)$, leading to better photosensitizers.[29] This approach has given Se-containing analogues of both chalcogenopyrylium dyes[30−32] and rhodamine dyes,[18−20,33] which all show increased phototoxicity relative to the S-containing analogues. The heavy-atom analogues of these DLCs still target the mitochondria of cells in culture.[30−33]

Herein, we describe the synthesis of the Se-containing analogues **15b**−**18b** (Chart 2) of the tetrahydroquinoline derivatives **15a**−**18a** and examine the utility of these compounds as photosensitizers for PDT in a murine colon carcinoma cell line expressing P-gp. The presence of the heavy Se atom imparts more desirable photophysical properties to the **15b**−**18b** relative to **15a**−**18a** including values of $\lambda_{max} > 600$ nm and values of $\Phi(^1O_2) \geq 0.44$. The thioamide analogues **16b** and **18b** also are useful in combination therapy involving PDT with the chemotherapeutic doxorubicin (Dox).

CHEMISTRY

Synthesis of Selenorhodamine Derivatives. Selenoxanthone **19** (Scheme 1), whose synthesis was recently described,[34] is the key intermediate for the preparation of selenorhodamine dyes **15b**−**18b**. Willgerodt−Kindler oxidation of thiophene-2-carboxaldehyde with elemental sulfur and diethylamine gave thioamide **20** in 49% isolated yield (Scheme 1).[28] Deprotonation of **20** with sterically bulky lithium diisopropylamide (LDA) gave the 2-thienyl anion **21** (Scheme 1), which was then added to a THF solution of selenoxanthone **19**. Workup with aqueous HPF_6 gave **16b** as the PF_6 salt in 81% isolated yield. Ion exchange with a chloride exchange resin converted **16b**-PF_6 to selenorhodamine **16b** as the Cl salt in 95% isolated yield (77% overall). The ^1H and ^{13}C NMR spectra

dx.doi.org/10.1021/jm501259v | J. Med. Chem. 2014, 57, 8622−8634

of Cl and PF_6 salts were superimposable. Unlike the tertiary amide group,[35] which is highly directing, the thioamide functionality does not direct lithiation in thiophenes. Only the more acidic α-proton of **20** was removed and none of the corresponding 2,3-disubstituted thiophene was detected in the product mixture.[36]

Similarly, Willgerodt−Kindler oxidation of thiophene-2-carboxaldehyde with elemental sulfur and piperidine gave thioamide **22** in 94% isolated yield.[28,37] Deprotonation of **22** with LDA gave 2-lithiothiophene **23** (Scheme 1), which was then added to a THF solution of **19**.[34] Workup with aqueous HPF_6 gave **18b**-PF_6 in 94% yield. Ion exchange with a chloride exchange resin converted **18b**-PF_6 to **18b** in 94% isolated yield (88% overall). The ^1H and ^{13}C NMR spectra of Cl and PF_6 salts were superimposable.

The PF_6 salts of thioamides **16b** and **18b** were converted to the PF_6 salts of amides **15b** and **17b** with trifluoroacetic anhydride in CH_2Cl_2.[28] Following workup, the intermediate salts were isolated as 5:1 and 3:1 mixtures, respectively, of the PF_6 and CF_3CO_2 salts based on the results of elemental analysis. The mixtures were subjected to ion exchange with a chloride exchange resin to give **15b** and **17b** in 55% and 98% overall yields, respectively, as a single salt. The ^1H and ^{13}C NMR spectra of Cl and PF_6 salts were superimposable.

Absorption Spectra. Absorption maxima (λ_{max}) and molar extinction coefficients (ε) in CH_3OH for **15a−18a**[28] and **15b−18b** are compiled in Table 1. Thiorhodamines **15a−18a** have values of λ_{max} of 597−598 nm, while **15b−18b** have values of λ_{max} of 608−609 nm with values of ε between 7.18×10^4 and 9.78×10^4 M^{-1} cm^{-1}. Values of λ_{max} for **15b−18b** are >600 nm and within the desired therapeutic window for PDT.[15] The electronic absorption spectra for **15b−18b** are compiled in Figure S1 (Supporting Information).

Fluorescence Yields. Steady-state fluorescence spectra for **15a−18a** and **15b−18b** were acquired in CH_3OH with excitation at 532 nm[17] using **3** in CH_3OH as a standard (Φ_{FL} = 0.93).[38] The thiorhodamines are fluorescent with Φ_{FL} of 0.07−0.09, while selenorhodamines **15b−18b** are weakly fluorescent ($\Phi_{FL} \leq 0.009$) because of the presence of Se as a heavy atom (Table 1). The fluorescence from **15b−18b** is still sufficient to visualize the dyes in cells as described below.

Singlet-Oxygen Yields. Values of $\Phi(^1O_2)$ for **15a−18a** and **15b−18b** were measured using time-resolved spectroscopy of $^1O_2$ luminescence at 1270 nm in air-saturated CH_3OH. Decay traces are compiled in Figure S2 in Supporting Information. Tetramethylselenorosamine hexafluorophosphate [$\Phi(^1O_2)$ = 0.87][17] was used as a standard. For **15b−18b**, values of $\Phi(^1O_2)$ fall in the range of 0.44−0.54 (Table 1). For **15a−18a**, the signal from $^1O_2$ luminescence could not be separated from background, suggesting values of $\Phi(^1O_2)$ of <0.05 (Table 1).

Photostability. Since the selenorhodamines produce $^1O_2$ efficiently, photobleaching of the dyes under conditions of continuous illumination could limit the utility of **15b−18b** as photosensitizers. Under conditions of continuous illumination with 350−800 nm light from a tungsten source delivered at 50 mW cm^{-2}, selenorhodamine thioamides **16b** and **18b** followed a first-order loss as a function of fluence with half of the dye chromophore lost after ~230 J cm^{-2} in solutions of 10% CH_3OH in pH 7.4 buffer as shown in Figure 1. If longer wavelengths of light were used, **18b** was more stable with half of the dye chromophore lost after ~850 J cm^{-2} of continuous illumination with 500−800 nm light in solutions of 10% CH_3OH in pH 7.4 buffer.

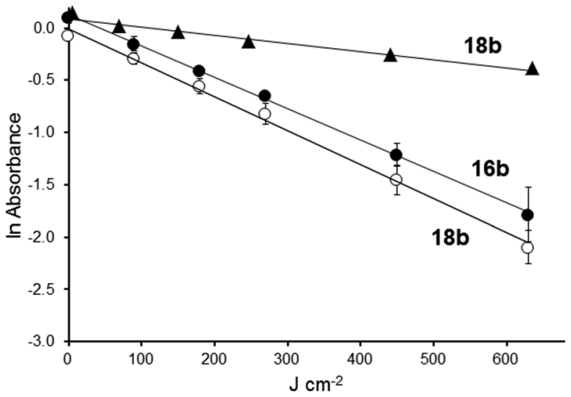

Figure 1. Photostability of **16b** (filled circles) and **18b** (open circles) toward 350−800 nm light delivered at 50 mW cm^{-2} and photostability of **18b** (filled triangles) toward 500−800 nm light delivered at 50 mW cm^{-2}. Error bars are ±SD.

***n*-Octanol/Water Partition Coefficients.** Experimental values of the *n*-octanol/water partition coefficient (log *P*) for **15b−18b** were measured using the "shake flask" method.[39] A saturated *n*-octanol solution of selenorhodamine was shaken with an equal volume of phosphate buffered saline (PBS) at pH 7.4, and the concentrations in the two layers were determined spectrophotometrically. Values of log *P* are compiled in Table 1 and covered a range from 1.61 for **18b** to 2.41 for **16b**. For comparison purposes, values of log *P* for **15a−18a**[28] are also compiled in Table 1. On the basis of this range of values of log *P*, **15b−18b** would have access to both aqueous and hydrophobic environments in the studies with whole cells described below.

BIOLOGY

Uptake of Rhodamines in the Presence of Verapamil in Colo-26 Cells. Colo-26 cells (a murine colon carcinoma cell line) express P-gp but are not deemed truly drug resistant.[40] Multidrug-resistance modifiers such as verapamil (VER) have shown significant effects in Colo-26 cells with respect to daunorubicin cytotoxicity, accumulation, and efflux.[41] We examined the uptake of **15a−18a** and **15b−18b** (0.5 μM) in Colo-26 cells incubated for 1 h with and without 100 μM VER by flow cytometry (Figures S3 and S4, Supporting Information). Results are shown in Figure 2 for mean fluorescence in the absence and presence of VER.

In the absence of VER, uptake of thioamides **16a**, **16b**, **18a**, and **18b** was significantly greater than the corresponding amide derivatives **15a**, **15b**, **17a**, and **17b** ($p < 0.02$ for all pairwise comparisons with Student *t* test) as shown in Figure 2. Uptake of **15a** increased more than 7-fold, and the uptake of **17a**, **15b**, and **17b** increased 5-fold in the presence of VER. In contrast, the uptake of thioamide derivative **18a** was essentially unchanged in the presence of VER while thioamides **16a**, **16b**, and **18b** only showed a 1.3- to 2-fold increase in uptake in the presence of VER. These data are consistent with (1) the presence of P-gp in the Colo-26 cells and (2) increased rates of transport of amide derivatives **15a**, **15b**, **17a**, and **17b** from Colo-26 cells relative to the thioamide-containing derivatives **16a**, **16b**, **18a**, and **18b**.

Dark and Phototoxicity of 15a−18a and 15b−18b toward Colo-26 Cells. Cell cultures of Colo-26 cells were

dx.doi.org/10.1021/jm501259v | J. Med. Chem. 2014, 57, 8622−8634

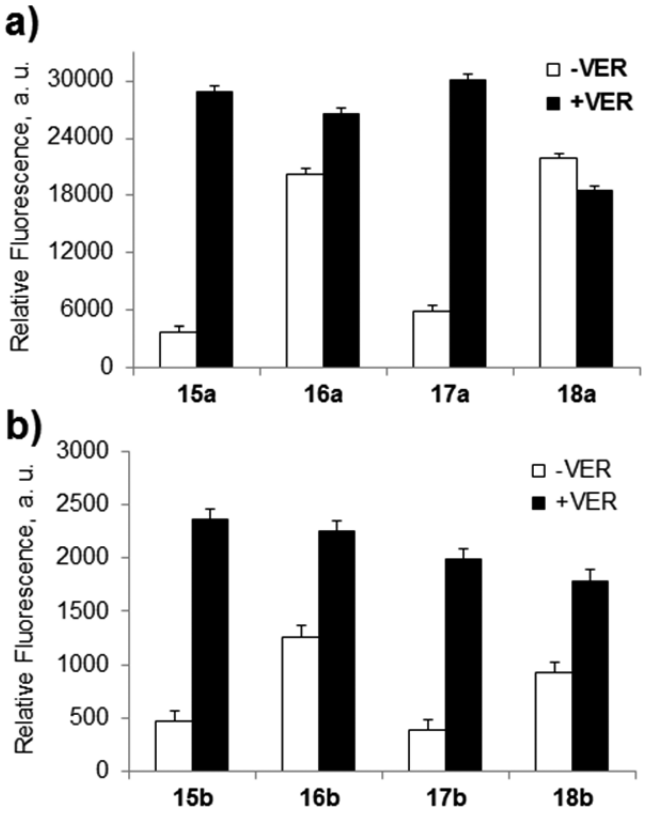

Figure 2. Uptake of (a) thiorhodamines **15a**–**18a** and (b) selenorhodamines **15b**–**18b** in Colo-26 cells as measured by relative fluorescence in the absence and presence of 100 μM verapamil (VER). Error bars represent the SD.

incubated for 1 h in the dark with various concentrations of **15a**–**18a** (0.1–0.5 μM). None of the dyes displayed any dark toxicity (surviving fraction of >0.95) at these concentrations. Light-treated cells and dark controls were incubated for 48 h, and cell survival was determined using the sulforhodamine B assay.[42,43] Thiorhodamines **15a**–**18a** displayed limited phototoxicity in Colo-26 cells incubated with dye concentrations of ≤0.5 μM and up to 1.0 J cm^{-2} of 350–700 nm light from a tungsten–halogen source (3.7–4.1 mW cm^{-2}) (Figure S5, Supporting Information). Compounds **15a**–**18a** were not investigated further as photosensitizers.

Phototoxicity of 15b–18b toward Colo-26 Cells with a Tunable Dye Laser Light Source. The phototoxicity of **15b**–**18b** toward Colo-26 cells was examined using a tunable dye laser delivering light at the absorption maximum (λ_{max} ± 2 nm). This approach allowed specific conditions to be tailored for each dye. In a solution of 17% fetal bovine serum (FBS) in PBS, values of λ_{max} for **15b**–**18b** were red-shifted 2–3 nm relative to values in CH_3OH. Colo-26 cells in 96-well plates were treated with varying concentrations of **15b**–**18b** (0.01–0.5 μM) and light (0.5 and 1.0 J cm^{-2}), which was delivered at λ_{max} (±2 nm) at a fluence rate of 3.2 mW cm^{-2}. The light-treated cells were then incubated with fresh medium for 48 h, and cell survival was determined for various concentrations of **15b**–**18b** and either a 0.5 or a 1.0 J cm^{-2} light dose, or for various light doses at 0.15 μM **15b**–**18b**. Dose–response curves for **18b** are summarized in Figure 3. Values of EC_{50} for 0.5 and 1.0 J cm^{-2} of light at λ_{max} are compiled in Table 2 (dose–response curves for **15b**–**17b**, Figure S6 in Supporting Information).

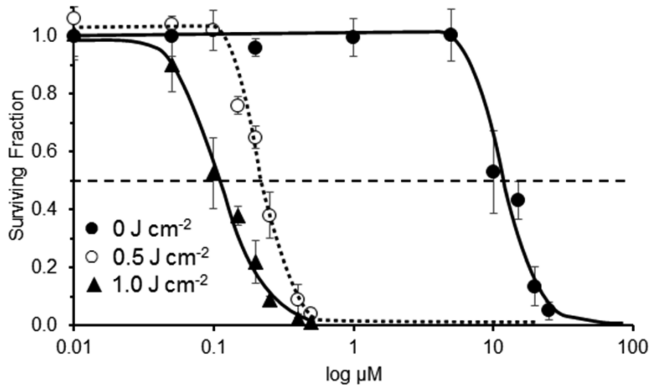

Figure 3. Dark toxicity (filled circles) of **18b** toward Colo-6 cells and phototoxicity of **18b** toward Colo-6 cells with irradiation from a tunable dye laser. Irradiation at 613 ± 2 nm was delivered at 3.2 mW cm^{-2} for varying concentrations of **18b** and 0.5 J cm^{-2} of light (open cicles) and 1.0 J cm^{-2} of light (filled triangles). Values of LD_{50} and EC_{50} were determined by sigmoidal dose–response (variable slope) analysis. Error bars are ±SD.

With 0.15 μM photosensitizer concentration and variable light dose as shown in Figure S6 (Supporting Information), thioamides **16b** and **18b** were comparably phototoxic with EC_{50} values of ∼1.0 J cm^{-2} of laser light. Amide **17b** showed little if any phototoxicity with 5.0 J cm^{-2} of laser light while 0.15 μM **15b** displayed some phototoxicity, but EC_{50} required >5.0 J cm^{-2} of light.

Dark Toxicity of 15b-18b toward Colo-26 Cells. The dark toxicity of **15b**–**18b** toward Colo-26 cells was examined at dye concentrations of 0.01–20 μM. Colo-26 cell cultures were incubated for 1 h in the dark with **15b**–**18b**. The medium was removed, and fresh medium was added. Cells were incubated for 48 h prior to determination of cell viability. Results are shown in Figure 3 for **18b** and in Figure S7 (Supporting Information) for **15b**–**17b** with sigmoidal dose–response (variable slope) analysis to allow values of LD_{50} (the concentration to give a surviving fraction of 0.50) with respect to dark toxicity to be determined for each dye. Values of LD_{50} are compiled in Table 2 as the mean of four replicates. The rank ordering of dark toxicity is **15b** > **18b** > **17b** > **16b** within the range of 7.8–9.5 μM. All pairwise comparisons were significantly different from one another ($p < 0.05$).

The ratio of dark toxicity to phototoxicity (as an approximation of the therapeutic ratio for the photosensitizers) could be a better measure of photosensitizer effectiveness. Values of LD_{50}/EC_{50} with 1.0 J cm^{-2} of laser light as a measure of therapeutic ratio are compiled in Table 2. Among **15b**–**18b**, amides **15b** and **17b** have lower LD_{50}/EC_{50} ratios of 22 and 26, respectively, relative to thioamides **16b** and **18b** with LD_{50}/EC_{50} ratios of 56 and 61, respectively.

P-gp Transport Studies of 11-Se–12-Se in Monolayers of MDCKII-MDR1 Cells. The interactions of the amide/thioamide pair **17b**/**18b** with P-gp were examined in monolayers of MDCKII-MDR1 cells, which overexpress P-gp.[44] Transport in this model approximates near-physiological conditions for studying P-gp–photosensitizer interactions.[44] The monolayers display apical and basolateral polarized membranes with P-gp solely present at the apical membrane. For **17b** and **18b**, transport was measured in the absorptive (P_{AB}) and secretory (P_{BA}) direction of the cell monolayer. Bovine serum albumin (BSA) addition to the buffer was required because a marked fraction of mass added to the donor

dx.doi.org/10.1021/jm501259v | J. Med. Chem. 2014, 57, 8622–8634

Table 2. EC_{50} Values for Selenorhodamines 15b−18b with Colo-26 cCells and 0.5 or 1.0 J cm^{-2} of Light (λ_{max} ± 2 nm), Dark Toxicities (LD_{50}), and Ratios of LD_{50}/EC_{50} with 1.0 J cm^{-2} of Light

	EC_{50},[a] ×10^{-7} M (λ_{max} ± 2 nm)[c]			
compd	0.5 J cm^{-2}	1.0 J cm^{-2}	LD_{50},[b] ×10^{-6} M (dark)	LD_{50}/EC_{50} (laser, 1.0 J cm^{-2})
15b	3.1 ± 0.1 (613 nm)	3.0 ± 0.1 (613 nm)	7.8 ± 0.4	26 ± 2
16b	2.0 ± 0.1 (611 nm)	1.7 ± 0.1 (611 nm)	9.5 ± 0.1	56 ± 4
17b	>5 (613 nm)	4.1 ± 0.1 (613 nm)	9.0 ± 0.1	22 ± 1
18b	2.2 ± 0.1 (611 nm)	1.4 ± 0.2 (611 nm)	8.5 ± 0.2	61 ± 10

[a]Mean of six determinations. Error limits are ±SD. [b]Mean of four determinations. Error limits are ±SD. [c]Values in parentheses are wavelengths of irradiation ± 2 nm.

equilibrated with the cell monolayer for **17b** and **18b**, resulting in gross underestimation of the permeability coefficient.[44] The assay was repeated with 5 μM **24** (LSN 335984, IC_{50} = 0.4 μM, Chart 3),[45] which completely inhibits P-gp. Compound **24** is

Chart 3. Structure of P-gp Inhibitor Used in Transport Studies

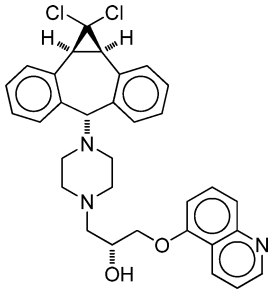

24 (LSN 335984)

related to the P-gp-specific inhibitor (*R*)-4-[(1a,6,10b)-1,1-difluoro-1,1*a*,6,10*b*-tetrahydrodibenzo[*a*,*e*]cyclopropa[*c*]-cyclohepten-6-yl][(5-quinolinyloxy)methyl]-1-piperazineethanol (LSN 335979, Chart 3).[4,45] Values of P_{AB} and P_{BA} in the absence of inhibitor, passive transport ($P_{Passive}$) in the fully inhibited system, and the % cell-associated dye in the AB direction in the absence or presence of inhibitor are compiled in Table 3. For comparison purposes, the same values are included in Table 3 for **17a** and **18a**.[28]

Selenorhodamines **17b** and **18b**, as well as **17a** and **18a**, are P-gp substrates with P_{BA}/P_{AB} ratios of >3.[2] This ratio is much larger for amide derivatives **17a** and **17b** (P_{BA}/P_{AB} of 228 and 182, respectively) relative to thioamide derivatives **18a** and **18b** (P_{BA}/P_{AB} of 38 and 15, respectively). For all seven compounds, $P_{Passive}$ is very slow: ≤6 × 10^{-9} m s^{-1}.

The % cell-associated dye was determined by a methanol wash of the cells in the monolayer following 1 h efflux in the AB direction. The trends observed in the % cell-associated dye indicate that the amide derivatives **17a** and **17b** show a much higher % cell-associated dye in the inhibited system relative to the uninhibited system (ratio of % cell ± inhibitor of 5.2 and 2.4, respectively, Table 3) relative to thioamide derivatives **18a** and **18b** (ratio of % cell ± inhibitor of 1.8 and 1.2, Table 3). These are the same trends as observed in the cellular uptake by flow cytometry of Colo-26 cells in the absence or presence of VER for **17a**/**18a** and **17b**/**18b**.[28]

Combination PDT and Chemotherapy. The ability of the selenorhodamines **15b**−**18b** to interact with P-gp in the Colo-26 cells should make it possible to do combination therapy involving PDT and a chemotherapeutic agent. Colo-26 cells were treated with combinations of Dox and **15b**−**18b** with and without light as shown in Figure 4 for **15b** and **16b** and in Figure S8 (Supporting Information) for **17b** and **18b**. In the dark, no synergy was observed between 0.15 μM **15b**−**18b** and various concentrations of Dox (0.005, 0.05, 0.5, 1.0, and 5.0 μM) and the surviving fraction was determined by the Dox concentration, with or without 0.15 μM photosensitizer (p > 0.05 for all pairwise comparisons). Irradiation of Colo-26 cells treated with 0.15 μM **15b** or **17b** with 1.0 J cm^{-2} of 613 nm laser light gave no significant phototoxicity (p > 0.05) relative to dark controls. No synergy was observed upon irradiation of Colo-26 cells with various concentrations of Dox in the presence of 0.15 μM **15b** or **17b**. All curves were essentially superimposable on Dox-only curves in the dark (Figures 4a and S8c).

Table 3. Transport and Cell Association Studies of Amide/Thioamide Pair 17b and 18b with MDCK-MDR1 Cells[a] and for Thiorhodamine Analogues 17a and 18a

compd	P_{AB}, ×10^{-9} m s^{-1}	P_{BA}, ×10^{-9} m s^{-1}	P_{BA}/P_{AB}	$P_{Passive}$,[b] ×10^{-9} m s^{-1}	% cell associated[c]	ratio (±inh)[d]
17a[e] (+inh)	≤1	230 ± 24	230		8.6 ± 0.1	5.2
	≤1	7.5 ± 0.1		~4	45 ± 1	
17b (+inh)	0.9 ± 0.3	164 ± 4	182		16 ± 1	2.4
	1.0 ± 0.1	11.1 ± 0.2		~6	39 ± 1	
18a[e] (+inh)	≤1	34 ± 22	34		34 ± 3	1.8
	≤1	0.2 ± 0.1		<1	62 ± 1	
18b (+inh)	1.9 ± 0.5	29 ± 3	15		45 ± 1	1.2
	1.7 ± 0.2	1.8 ± 0.1		~2	55 ± 1	

[a]Experiments were run with 5 μM dye and 4.3 mg mL^{-1} BSA. Values of transport in the absorptive (P_{AB}) and secretory (P_{BA}) mode in the absence or presence of inhibitor, the ratio P_{BA}/P_{AB}, the % cell associated rhodamine analogue in the absence or presence of inhibitor, and the ratio of cell associated rhodamine in the presence or absence of inhibitor are reported. Details for methods are provided in Experimental Section. Error limits are ± SD. [b]$P_{Passive}$ represents the mean of P_{AB} and P_{BA} in the fully inhibited system. [c]% cell associated is the fraction of mass extracted from the cell monolayer by methanol wash after a 1 h flux in the AB direction. [d]For % cell associated dye. [e]Values from ref 28.

dx.doi.org/10.1021/jm501259v | J. Med. Chem. 2014, 57, 8622−8634

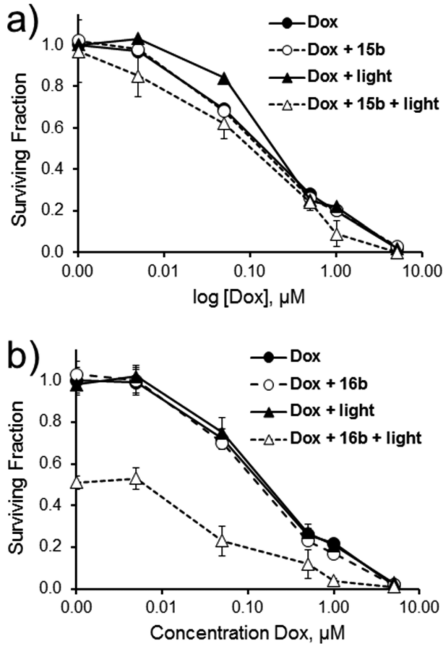

Figure 4. Combination treatment of Colo-26 cells with various concentrations of Dox alone or in combination with (a) **15b** (0.15 μM) and (b) **16b** (0.15 μM) in the dark or with 1.0 J cm^{-2} of 613 nm light (for **15b**) or 611 nm light (for **16b**). Values are the mean of six replicates. Error bars are ±SD.

In contrast, cells treated with 0.15 μM **16b** or **18b** and 1.0 J cm^{-2} of 611 nm light displayed some phototoxicity upon irradiation with 1.0 J cm^{-2} of 611 nm light in the absence of Dox (Figures 4b and S8d, respectively). Colo-26 cells treated with 0.15 μM photosensitizer, 1.0 J cm^{-2} of 611 nm light, and 0.5 μM Dox showed a statistically significant decrease in pairwise comparisons to Dox-only treatment with and without light, photosensitizer-only treatment with and without light, and photosensitizer and Dox treatment in the dark ($p \leq 0.0079$ for **18b** in pairwise comparisons and $p \leq 0.0064$ for **16b** in pairwise comparisons). Statistically significant differences in surviving fraction were also noted with 1.0 μM Dox and **16b** or **18b**, but the surviving fraction was ≤0.20 for these combinations, which was very similar to the Dox-only treatment (minimizing the impact of PDT).

Localization of 15b−18b in the Mitochondria of Colo-26 Cells. Rhodamine dyes such as **2** and **3** (Chart 1) are concentrated in the mitochondria of cancer cells because of the increased mitochondrial membrane potential in the transformed cells.[10,11] While one would expect a similar pattern with selenorhodamines **15b−18b**, ImageStream flow cytometry demonstrated mitochondrial targeting in Colo-26 cells by these agents as shown in Figure 5. A statistical analysis of the similarity of localization of the mitochondrial specific agents 9-[4-(chloromethyl)phenyl]-2,3,6,7,12,13,16,17-octahydro-[1*H*,5*H*,11*H*,15*H*]xantheno[2,3,4-*ij*:5,6,7-*i*′*j*′]diquinolizin-18-ium chloride (**25** or MTG, Chart 4) and 9-[4-(chloromethyl)-phenyl]-2,3,6,7,12,13,16,17-octahydro[1*H*,5*H*,11*H*,15*H*]xantheno[2,3,4-*ij*:5,6,7-*i*′*j*′]diquinolizin-18-ium chloride (**26** or MTR) in Colo-26 cells incubated with both agents gave a

Chart 4. Structures of 25 (MTG), 26 (MTR), and 27 (LYS)

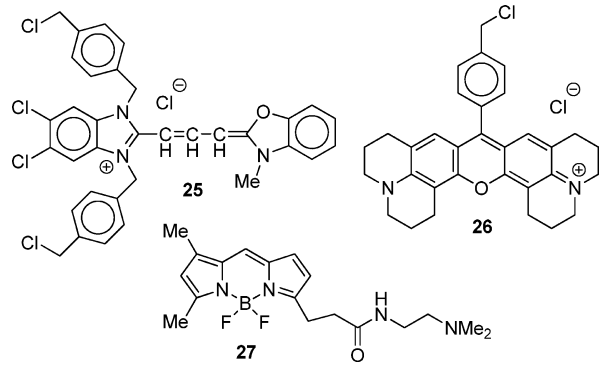

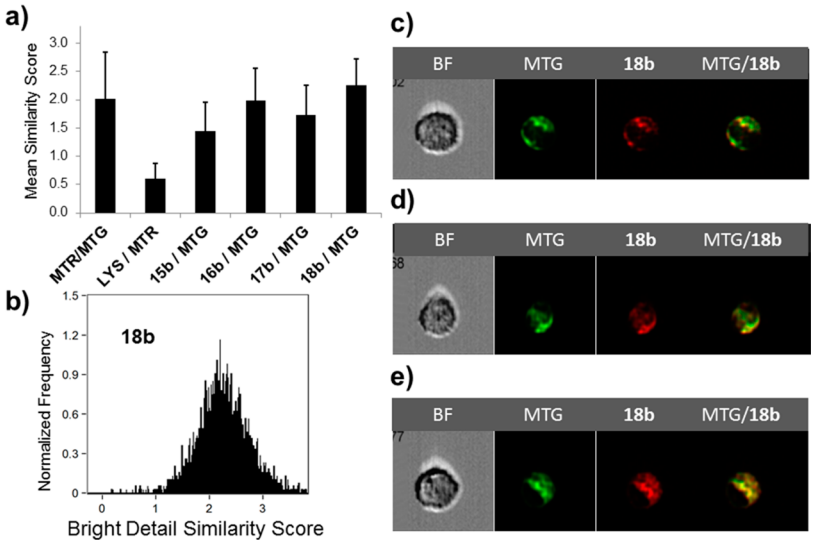

Figure 5. (a) The average similarity coefficient determined by ImageStream flow cytometry of all cells for each pair of agents (MTR, MTG, LYS, **15b−18b**) is shown; error bars represent SD. (b) Histogram of the pixel-by-pixel statistical analysis of each cell (n = 3900) analyzed, in which the y-axis is number of cells and the x-axis is the similarity coefficient between MitoTracker Green and **18b**. Shown are representative examples of **18b**/MTG-stained Colo-26 cells as a bright field image (BF), MTG fluorescence, **18b** fluorescence, and a merged image of MTG/**18b** fluorescence for cells with (c) low similarity, (d) intermediate similarity, and (e) high similarity.

dx.doi.org/10.1021/jm501259v | J. Med. Chem. 2014, 57, 8622−8634

mean bright detail similarity score of 2.0 ± 0.8 for 1300 cells, indicating a high degree of colocalization[46] of these two agents (Figure 5a). In contrast, Colo-26 cells incubated with the lysosome-specific 3-(5,5-difluoro-7,9-dimethyl-5*H*-4λ^4,5λ^4-dipyrrolo[1,2-*c*:2′,1′-*f*][1,3,2]diazaborinin-3-yl)-*N*-(2-(dimethylamino)ethyl)propanamide (**27** or LYS, Chart 4) and MTR gave a much lower bright detail similarity score of 0.6 ± 0.3 for 2000 cells, indicating that MTR and LYS do not localize to the same places in the cell (Figure 5a).

Colo-26 cells were next incubated for 15 min with a dye solution consisting of MTG and 0.2 μM **15b**−**18b**. ImageStream flow cytometry gave the **15b**−**18b**/MTG bright detail similarity scores shown in Figure 5a alongside a comparison with the MTR/MTG and LYS/MTR similarity scores. Similarity scores in the range 1.4−2.3 suggest that **15b**−**18b** colocalize with MTG.

The histogram of Figure 5b provides an analysis of the similarity of localization of MTG and **18b**. The individual cells shown in Figure 5c−e represent examples of low similarity, intermediate similarity, and high similarity, respectively, for localization of **18b** and MTG. Similar data (cell images, histograms of similarity scores) for selenorhodamines **15b** and **16b** are compiled in Figure S9of Supporting Information and for selenorhodamine **17b** in Figure S10.

DISCUSSION

Our initial interest in heavy-chalcogen analogues of the various rhodamines/rosamines was as photosensitizers for use in PDT[20,33] and for the photodynamic inactivation of viral and bacterial pathogens in blood.[47,48] We found that chalcogenorhodamines with a 2-thienyl substituent in the 9-position gave values of $\lambda_{max} \geq 20$ nm longer than chalcogenorhodamines with a 9-phenyl substituent.[49] Another exciting observation was the efficacy of the Se-analogue of **6** (Chart 1) as a photosensitizer toward MDR cells.[33] The added lipophilicity from the julolidyl fragment was thought to be important with respect to efficacy in MDR cells. This observation led to the screening of numerous chalcogenorhodamines as modulators/inhibitors of P-gp with the intent of developing efficient photosensitizers for use with MDR cells. Among the rhodamine libraries that we examined, several structures emerged as modulators of P-gp ATPase activity and have increased the cellular uptake of agents such as CAM and vinblastine into MDR cells.[27,28]

Impact of Structure on Physical and Photophysical Properties. The structural characteristics of the best rhodamine modulators include the incorporation of the julolidine fragment (**11a**−**14a**, Chart 2) or the tetrahydroquinoline fragment (**15a**−**18a**, Chart 2). A second structural feature is the presence of the thioamide functionality (**12a**, **14a**, **16a**, and **18a**, Chart 2) which decreases or inhibits P-gp ATPase activity relative to the amide structures (**11a**, **13a**, **15a**, and **17a**). Those incorporating the tetrahydroquinoline fragment were better modulators than those incorporating the julolidine fragment based on values of IC_{50} for uptake of CAM.[28]

A structural feature with little impact on P-gp modulation is the chalcogen atom in the rhodamine core. Thioamide **10a** and its Se-analogue have comparable values of IC_{50} for CAM uptake as do thioamide **14a** and its Se-analogue.[28] Thus, photosensitizer photophysical properties can be optimized via the chalcogen atom without major consequence to P-gp modulation.

Selenorhodamines **15b**−**18b** were designed to have improved physical and photophysical properties as photosensitizers (Table 1) relative to thiorhodamines **15a**−**18a**. Because of the incorporation of a 2-thienyl substituent at the 9-position and the incorporation of the Se atom in the xanthylium core, selenorhodamines **15b**−**18b** have values of λ_{max} > 600 nm, absorb light strongly at λ_{max} ($\varepsilon = 7.18 \times 10^4$ to 9.78×10^4 M^{-1} cm^{-1}), and generate $^1O_2$ efficiently [$\Phi(^1O_2)$ = 0.44−0.54]. The thioamides **16b** and **18b** are reasonably photostable at pH 7.4 with half-lives of ∼230 J cm^{-2} for exposure to 350−800 nm light and, for **18b**, ∼850 J cm^{-2} for exposure to 500−800 nm light (Figure 1). The range of values of log *P* (1.61−2.41) for **15b**−**18b** suggests that these molecules should have access to both aqueous and hydrophobic environments in the cell.

Interactions with P-gp and the Amide/Thioamide Switch. The biological properties of **15b**−**18b** also suggest that thioamides **16b** and **18b** should be excellent photosensitizer candidates. The amide/thioamide switch appears to be operative in this series of compounds with respect to stimulation/inhibition of P-gp ATPase activity. In Colo-26 cells, the uptake of amide derivatives **15b** and **17b** is increased 5-fold in the presence of 100 μM VER while uptake of thioamides **16b** and **18b** increased only 2-fold (Figure 2). Higher accumulation of the **16b** and **18b** is likely a consequence of partial inhibition of P-gp, while amides **15b** and **17b** stimulate ATPase activity.

Increased uptake of thioamide **18b** relative to amide **17b** was also demonstrated in monolayers of MDCKII-MDR1 cells. The % cell-associated dye in cells treated with thioamide **18b** (45%, Table 3) was more than 2-fold higher relative to amide **17b**-treated cells (16%, Table 3). In the presence of inhibitor, % cell-associated dye was essentially unchanged with thioamide **18b** (45−55% with inhibitor; ratio ± inhibitor of 1.2, Table 3) but increased by a factor of 2.4 in the presence of inhibitor for cells treated with amide **17b** (16−39%, Table 3). These results again suggest that higher accumulation in the thioamide-treated cells is likely due to partial inhibition of P-gp by thioamide **18b**. If one examines rates of absorptive (P_{AB}) and secretory (P_{BA}) transport, values of P_{AB} for **17b** and **18b**, as well as their thiorhodamine counterparts **17a** and **18a**, are nearly identical: $\sim(1-2) \times 10^{-9}$ m s^{-1}. However, values of P_{BA} are much higher for amides **17a** and **17b** (230×10^{-9} and 182×10^{-9} m s^{-1}, respectively) relative to thioamides **18a** and **18b** (34×10^{-9} and 15×10^{-9} m s^{-1}, respectively), which is again consistent with exclusion of the amides to a greater extent than the thioamides.

Efficacy of 15b−18b as Photosensitizers. With higher accumulation of **16b** and **18b** in P-gp-expressing cells, thioamides **16b** and **18b** appear to be better photosensitizers than their amide counterparts **15b** and **17b**. The thioamides **16b** and **18b** have lower values of EC_{50} than amides **15b** and **17b**, and thioamide-treated cells also show a lower surviving fraction than amide-treated cells for a given photosensitizer concentration and light dose (Table 2). With 1.0 J cm^{-2} of laser light (λ_{max} ± 2 nm), thioamides **16b** and **18b** have values of EC_{50} of 0.17 and 0.14 μM, respectively. To put these values in perspective, the selenopyrylium analogue of **4** (Chart 1) and closely related structures give values of EC_{50} of 0.07 M to 0.37 μM toward Colo-26 cells with 15 J cm^{-2} of 360−800-nm light.[31] Toward different cell lines, the selenium analogue of **6** (Chart 1) required 5 J cm^{-2} of 350−800-nm light to give an EC_{50} of 0.1 μM.

The dark toxicity of **15b**−**18b** toward Colo-26 cells gave values of LD_{50} of 7.8 to 9.5 μM, which is a much lower dark

dx.doi.org/10.1021/jm501259v | J. Med. Chem. 2014, 57, 8622−8634

toxicity than observed with related cationic photosensitizers. Values of LD_{50} for thiopyrylium dye **4** (Chart 1) and closely related structures toward Colo-26 cells are 0.1−2.6 μM.[32] When the dark toxicity of **16b** and **18b** is combined with the very low values of EC_{50}, the therapeutic ratio between dark and phototoxicity is >55 for these two dyes (Table 2).

Like other rhodamines, **15b**−**18b** appear to target the mitochondria of cells. As shown in Figure 5, the average similarity coefficients determined by image streamflow cytometry are in the range 1.4−2.3 in comparison of selenorhodamine localization with MTG localization. Similarity scores of >1.0 are indicative of colocalization of agents.[46] The overlay of emission from MTG with emission from **18b** is also readily apparent in Figure 5c−e.

The amide derivatives **15b** and **17b** had low dark toxicity and also target mitochondria in the Colo-26 cells but were less efficient as photosensitizers than the thioamide derivatives. As shown in Figure 2, the uptake of **15b** and **17b** was roughly 40−50% of the corresponding thioamide derivatives. The reduced phototoxicity is easily understood. However, the amide derivatives are still interacting with P-gp in the Colo-26 cells and irradiation of **15b** or **17b**-treated cells may damage P-gp even though cellular phototoxicity is reduced.

Potential for Combination Therapy. The anthracycline anticancer drug Dox, while useful for the treatment of many malignancies,[50,51] suffers from the side effect of cardiotoxicity, which may limit its clinical use.[51,52] The onset of cardiomyopathy can be quite rapid, occurring within 2−3 days following Dox administration.[52]

The combination therapy of PDT with thioamides **16b** and **18b** along with coadministration of Dox shows synergistic effects as illustrated in Figures 4 and S8 (Supporting Information). The combination of 0.15 μM photosensitizer, 0.05 μM Dox, and 1.0 J cm^{-2} of light gives a surviving fraction that is equivalent to 0.15 μM photosensitizer and 2 J cm^{-2} of light in the absence of Dox (Figure S6c) or that is equivalent to 0.5 μM Dox in the absence of **16b** or 0.3 μM Dox in the absence of **18b** (Figures 3b and S8d, respectively). These encouraging results suggest that animal studies to test the combination therapy would be appropriate.

The amide analogues **15b** and **17b** do not show significant synergistic effects. The active transport of these photosensitizers by P-gp from the Colo-26 cells is likely responsible for the difference in results with amide and thioamide subsets.

CONCLUSIONS

The incorporation of a selenium atom in the xanthylium core of the rhodamines and a 2-thienyl substituent at the 9-position of the rhodamines and the locking of one nitrogen atom into conjugation with the xanthylium core provide selenorhodamines with values of λ_{max} > 600 nm and with values of $\Phi(^1O_2) \geq 0.44$. Both of these attributes are desirable characteristics for photosensitizers for the photodynamic therapy of cancer. The family of selenorhodamines **15b**−**18b** targets the mitochondria of Colo-26 cells as determined by colocalization studies with MTG. The mitochondria are cellular targets of DLCs used as photosensitizers for PDT.[15] Within this family, thioamide analogues **16b** and **18b** modulate/inhibit P-gp expressed by the Colo-26 cells, allowing increased uptake of the thioamides relative to amide analogues **15b** and **17b**. The thioamides are effective photosensitizers against P-gp-expressing cells and have the potential to be used in combination therapy with other chemotherapeutic agents. Subsequent animal studies to examine efficacy in vivo are ongoing.

EXPERIMENTAL SECTION

General Methods. Selenoxanthone **19** was prepared by literature methods.[34] Thiorhodamines **15a**−**18a** were prepared by literature methods.[28] Reactions were run under Ar. Tetrahydrofuran was distilled from sodium benzophenone ketyl prior to use. Concentration in vacuo was performed on a Büchi rotary evaporator. NMR spectra were recorded on an Inova 500 instrument (500 MHz for ^1H, 125 MHz for ^{13}C) with residual solvent signal as internal standard. Infrared spectra were recorded on a PerkinElmer FTIR instrument. UV−vis−near-IR spectra were recorded on a PerkinElmer Lambda 12 spectrophotometer or on a Shimadzu UV-3600 spectrophotometer in quartz cuvettes with a 1 cm path length. Melting points were determined with a Büchi capillary melting point apparatus and are uncorrected. All compounds tested have a purity of at least 95%, which was determined from NMR spectra (Supporting Information) or by elemental analyses for C, H, and N (Atlantic Microlab, Inc., Norcross, GA). Experimental values of C, H, and N are within 0.4% of theoretical values.

Preparation of 9-(5-(Diethylcarbamothioyl)thiophen-2-yl) Selenorhodamine 16b. *n*-Butyllithium (1.38 M in hexanes, 1.92 mL, 2.93 mmol) was added dropwise to a stirred solution of *N*,*N*-diisopropylamine (0.500 mL, 3.53 mmol) in THF (10 mL) at −78 °C. The resulting mixture was stirred for 10 min before it was transferred to a stirred solution of *N*,*N*-diethylthiophene-2-carbothioamide (599 mg, 3.00 mmol) in THF (60 mL) at −78 °C. The resulting solution was stirred at −78 °C for 2 min before it was transferred via cannula to a stirred solution of selenoxanthone **19** (300 mg, 0.751 mmol, 1.0 equiv) in THF (30 mL) at room temperature. The resulting solution was heated to 45 °C for 0.5 h before it was cooled to ambient temperature. Glacial acetic acid (2 mL) was added, and the resulting mixture was poured into 10% aqueous HPF_6 at 0 °C. The resulting mixture was stirred 12 h, and the precipitate was collected via filtration and then washed with water (50 mL) and diethyl ether (100 mL). The product was purified via column chromatography (SiO_2, 6% MeOH/CH_2Cl_2, R_f = 0.4), followed by recrystallization from ether/CH_2Cl_2 to yield 441 mg (81%) of **16b**-PF_6 as a purple solid, mp 226−229 °C. ^1H NMR (500 MHz, CD_2Cl_2) δ 7.80 (d, 1 H, *J* = 10.0 Hz), 7.59 (s, 1 H), 7.26−7.20 (m, 2 H), 7.19 (s, 1 H), 7.05 (d, 1 H, *J* = 4.0 Hz), 6.93 (dd, 1 H, *J* = 2.0, 10.0 Hz), 4.12 (br s, 2 H), 3.86 (br s, 2 H), 3.60 (t, 2 H, J = 6.0 Hz), 3.27 (s, 3 H), 3.25 (s, 6 H), 1.79 (t, 2 H, *J* = 6.0 Hz), 1.39 (t, 6 H, *J* = 6.5 Hz), 1.67 (s, 6 H); ^{13}C NMR (500 MHz, CD_2Cl_2) δ 189.0, 153.1, 152.2, 150.8, 148.9, 145.1, 144.7, 139.6, 137.9, 135.4, 132.4, 130.0, 124.6, 121.2, 120.6, 115.2, 109.0, 108.4, 49.1, 48.0 (br), 40.9, 40.4, 34.6, 32.3, 28.6; HRMS (ESI, HRDFMagSec) *m*/*z* 582.1511 (calcd for $C_{30}H_{36}N_3S_2{}^{80}Se^+$, 582.1510). Anal. Calcd for $C_{30}H_{36}N_3S_2Se{\cdot}PF_6$: C, 49.59; H, 4.99; N, 5.78. Found: C, 49.95; H, 5.10; N, 5.84.

The hexafluorophosphate salt **16b**-PF_6 (25.0 mg, 0.0344 mmol) was dissolved in CH_2Cl_2 (10 mL), and Amberlite IRA-400 chloride ion-exchange resin (3.0 g) was added. The mixture was stirred at ambient temperature for 24 h. The Amberlite exchange resin was removed via filtration, and the filtrate was concentrated under reduced pressure. The process was repeated two additional times, yielding 20.1 mg (95%, 77% overall) of **16b** as the chloride salt. ^1H NMR (500 MHz, CD_2Cl_2) δ 7.80 (d, 1 H, *J* = 10.0 Hz), 7.59 (s, 1 H), 7.26−7.20 (m, 2 H), 7.19 (s, 1 H), 7.05 (d, 1 H, *J* = 4.0 Hz), 6.93 (dd, 1 H, *J* = 2.0, 10.0 Hz), 4.12 (br s, 2 H), 3.86 (br s, 2 H), 3.60 (t, 2 H, *J* = 6.0 Hz), 3.27 (s, 3 H), 3.25 (s, 6 H), 1.79 (t, 2 H, *J* = 6.0 Hz), 1.39 (t, 6 H, *J* = 6.5 Hz), 1.67 (s, 6 H); ^{13}C NMR (500 MHz, CD_2Cl_2) δ 189.0, 153.1, 152.2, 150.8, 148.9, 145.1, 144.7, 139.6, 137.9, 135.4, 132.4, 130.0, 124.6, 121.2, 120.6, 115.2, 109.0, 108.4, 49.1, 48.0 (br), 40.9, 40.4, 34.6, 32.3, 28.6; IR (film on NaCl) 1592, 1506, 1472, 1446, 1407, 1386, 1356, 1329, 1254, 1212 cm^{-1}; λ_{max} (MeOH) 608 nm ($\varepsilon = 8.63 \times 10^4$ M^{-1} cm^{-1}); HRMS (ESI, HRDFMagSec) *m*/*z* 582.1511 (calcd for $C_{30}H_{36}N_3S_2{}^{80}Se^+$, 582.1510). Anal. Calcd for $C_{30}H_{36}N_3S_2SeCl{\cdot}4H_2O$: C, 52.28; H, 6.44; N, 6.10. Found: C, 52.33; H, 6.41; N, 6.18.

dx.doi.org/10.1021/jm501259v | J. Med. Chem. 2014, 57, 8622−8634

Preparation of 9-(5-(Diethylcarbamoyl)thiophen-2-yl) Selenorhodamine 15b. Trifluoroacetic anhydride (0.308 mL, 2.22 mmol) was slowly added to a stirred solution of hexafluorophosphate salt of **16b** (161 mg, 0.222 mmol) in CH_2Cl_2 (30 mL). The resulting mixture was heated at reflux for 12 h and then cooled to ambient temperature. A solution of 10% aqueous Na_2CO_3 (20 mL) was added, and the mixture was extracted with CH_2Cl_2 (3 × 25 mL). The combined organic extracts were dried over anhydrous $MgSO_4$, filtered, and concentrated. The resulting product was purified via recrystallization in ether/CH_2Cl_2 to give **15b**-PF_6 as a 5:1 mixture of presumably the hexafluorophosphate and trifluoroacetate salts as a blue solid. ^{1}H NMR (500 MHz, CD_3CN) δ 7.63 (d, 1 H, J = 9.5 Hz), 7.52−7.46 (m, 2 H), 7.38 (d, 1 H, J = 2.5 Hz), 7.35 (s, 1 H), 7.17 (d, 1 H, J = 3.5 Hz), 6.96 (dd, 1 H, J = 2.5, 9.5 Hz), 3.56 (t, 6 H, J = 6.0 Hz), 3.21 (s, 3 H), 3.19 (s, 6 H), 1.74 (t, 2 H, J = 6.0 Hz), 1.25 (t, 6 H, J = 7.0 Hz), 1.10 (s, 6 H); ^{13}C NMR (300 MHz, $CDCl_3$) δ 162.5, 152.4, 151.1, 150.2, 145.2, 144.7, 141.3, 139.7, 137.2, 135.0, 131.6, 129.9, 127.9, 120.7, 120.0, 114.7, 108.8, 108.4, 48.5, 42.5 (br), 40.6, 40.3, 34.2, 31.8, 28.5; HRMS (ESI, HRDFMagSec) m/z 566.1745 (calcd for $C_{30}H_{36}N_3OS^{80}Se^+$, 566.1739). Anal. Calcd for $C_{30}H_{36}N_3OSSe\cdot(^5/_6PF_6 + {}^1/_6CF_3CO_2)$: C, 51.66; H, 5.15; N, 5.96. Found: C, 51.36; H, 5.27; N, 5.96.

15b-PF_6 was converted to the chloride salt as described for the preparation of **16b** to give **15b** (68.6 mg, 44% overall) as a blue solid, mp 144−147 °C. ^{1}H NMR (500 MHz, CD_3CN) δ 7.63 (d, 1 H, J = 9.5 Hz), 7.52−7.46 (m, 2 H), 7.38 (d, 1 H, J = 2.5 Hz), 7.35 (s, 1 H), 7.17 (d, 1 H, J = 3.5 Hz), 6.96 (dd, 1 H, J = 2.5, 9.5 Hz), 3.56 (t, 6 H, J = 6.0 Hz), 3.21 (s, 3 H), 3.19 (s, 6 H), 1.74 (t, 2 H, J = 6.0 Hz), 1.25 (t, 6 H, J = 7.0 Hz), 1.10 (s, 6 H); ^{13}C NMR (300 MHz, $CDCl_3$) δ 162.5, 152.4, 151.1, 150.2, 145.2, 144.7, 141.3, 139.7, 137.2, 135.0, 131.6, 129.9, 127.9, 120.7, 120.0, 114.7, 108.8, 108.4, 48.5, 42.5 (br), 40.6, 40.3, 34.2, 31.8, 28.5; IR (film on NaCl) 1591, 1447, 1386, 1328, 1254 cm^{-1}; λ_{max} (MeOH) 609 nm (ε = 1.04 × 10^5 M^{-1} cm^{-1}); HRMS (ESI, HRDFMagSec) m/z 566.1745 (calcd for $C_{30}H_{36}N_3OS^{80}Se^+$, 566.1739). Anal. Calcd for $C_{30}H_{36}N_3OSSeCl\cdot4H_2O$: C, 53.53; H, 6.59; N, 6.24. Found: C, 53.52; H, 6.47; N, 6.27.

Preparation of 9-(5-(Piperidylcarbamothioyl)thiophen-2-yl) Selenorhodamine 18b. *n*-Butyllithium (1.38 M in hexanes, 2.34 mL, 2.93 mmol), *N*,*N*-diisopropylamine (0.490 mL, 3.53 mmol), piperidin-1-yl(thiophen-2-yl)methanethione (635 mg, 3.00 mmol), and selenoxanthone **19** (300 mg, 0.751 mmol) in THF (10 and 60 mL) were treated as described for the preparation of **16b** to give 0.521 g (94%) of **18b**-PF_6, mp 233−236 °C. ^{1}H NMR (500 MHz, CD_2Cl_2) δ 7.82 (d, 1 H, J = 9.5 Hz), 7.56 (s, 1 H), 7.23 (d, 1 H, J = 2.0 Hz), 7.22−7.17 (m, 2 H), 7.06 (d, 1 H, J = 3.5 Hz), 6.93 (dd, 1 H, J = 9.5, 2.0 Hz), 4.30 (broad s, 2 H), 3.99 (broad s, 2 H), 3.60 (t, 2 H, J = 6.0 Hz), 3.27 (s, 3 H), 3.25 (s, 6 H), 1.79 (t, 8 H, J = 6.0 Hz), 1.16 (s, 6 H); ^{13}C NMR (300 MHz, $CDCl_3$) δ 188.5, 162.2, 152.7, 151.3, 150.4, 148.1, 145.1, 145.0, 144.6, 140.6, 139.6, 139.4, 137.6, 137.4, 135.1, 131.8, 129.9, 129.7, 125.1, 120.7, 120.1, 115.0, 108.7, 108.3, 48.6, 40.5, 40.2, 34.3, 31.9, 28.5, 26.2, 24.5, 24.1, with splitting due to isomerization; HRMS (ESI, HRDFMagSec) m/z 594.1505 (calcd for $C_{31}H_{36}N_3S_2{}^{80}Se^+$, 594.1510). Anal. Calcd for $C_{31}H_{36}N_3S_2Se\cdot PF_6$: C, 50.41; H, 4.91; N, 5.69. Found: C, 50.58; H, 5.04; N, 5.64.

The **18b**-PF_6 (0.521 g, 0.706 mmol) was treated with Amberlite IRA-400 chloride as described for the preparation of **16b** to yield the chloride salt **18b** (418 mg, 94%) as a blue solid, mp 233−236 °C. ^{1}H NMR (500 MHz, CD_2Cl_2) δ 7.82 (d, 1 H, J = 9.5 Hz), 7.56 (s, 1 H), 7.23 (d, 1 H, J = 2.0 Hz), 7.22−7.17 (m, 2 H), 7.06 (d, 1 H, J = 3.5 Hz), 6.93 (dd, 1 H, J = 9.5, 2.0 Hz), 4.30 (broad s, 2 H), 3.99 (broad s, 2 H), 3.60 (t, 2 H, J = 6.0 Hz), 3.27 (s, 3 H), 3.25 (s, 6 H), 1.79 (t, 8 H, J = 6.0 Hz), 1.16 (s, 6 H); ^{13}C NMR (300 MHz, $CDCl_3$) δ 188.5, 162.2, 152.7, 151.3, 150.4, 148.1, 145.1, 145.0, 144.6, 140.6, 139.6, 139.4, 137.6, 137.4, 135.1, 131.8, 129.9, 129.7, 125.1, 120.7, 120.1, 115.0, 108.7, 108.3, 48.6, 40.5, 40.2, 34.3, 31.9, 28.5, 26.2, 24.5, 24.1, with splitting due to isomerization; IR (film on NaCl) 2936, 2360, 1592, 1508, 1474, 1445, 1407, 1386, 1328, 1254, 1213 cm^{-1}; λ_{max} (MeOH) 608 nm (ε = 1.16 × 10^5 M^{-1} cm^{-1}); HRMS (ESI, HRDFMagSec) m/z 594.1505 (calcd for $C_{31}H_{36}N_3S_2{}^{80}Se^+$, 594.1510). Anal. Calcd for $C_{31}H_{36}N_3S_2SeCl\cdot4H_2O$: C, 53.10; H, 6.32; N, 5.99. Found: C, 53.35; H, 6.17; N, 6.04.

Preparation of 9-(5-(Piperidylcarbamoyl)thiophen-2-yl) Selenorhodamine 17b. Trifluoroacetic anhydride (0.380 mL, 2.71 mmol) and the PF_6 salt of **18b** (200 mg, 0.271 mmol) in CH_2Cl_2 (30 mL) were treated as described for the preparation of **15b** to give the PF_6 salt, mp 194−197 °C. ^{1}H NMR (500 MHz, CD_2Cl_2) δ 7.72 (d, 1 H, J = 10.0 Hz), 7.52 (s, 1 H), 7.41 (d, 1 H, J = 3.5 Hz), 7.35−7.24 (m, 2 H), 7.13 (d, 1 H, J = 3.5 Hz), 6.89 (d, 1 H, J = 9.0 Hz), 3.72 (t, 4 H, J = 5.0 Hz), 3.60 (t, 2 H, J = 5.0 Hz), 3.29 (s, 3 H), 3.25 (s, 6 H), 1.82−1.72 (m, 4 H), 1.71−1.64 (m, 4 H), 1.14 (s, 6 H); ^{13}C NMR (300 MHz, $CDCl_3$) δ 162.1, 152.5, 151.1, 150.2, 145.1, 144.7, 140.4, 139.4, 137.3, 135.0, 131.6, 129.8, 128.2, 120.7, 120.0, 114.8, 108.7, 108.3, 48.5, 40.6, 40.2, 34.2, 31.8, 28.5, 26.1, 24.5; IR (film on NaCl) 2936, 2859, 1592, 1536, 1508, 1473, 1446, 1408, 1387, 1329, 1255, 1214 cm^{-1}; HRMS (ESI, HRDFMagSec) m/z 578.1739 (calcd for $C_{31}H_{36}N_3OS^{80}Se^+$, 578.1739). Anal. Calcd for $C_{31}H_{36}N_3OSSe\cdot(^2/_3PF_6 + {}^1/_3CF_3CO_2)$: C, 52.63; H, 5.02; N, 5.81. Found: C, 52.55; H, 5.18; N, 5.75.

The PF_6 salt **17b**-PF_6 was treated with Amberlite IRA-400 chloride as described for the preparation of **16b** to yield 192 mg (98%) of chloride salt **17b** as a blue solid, mp 194−197 °C. ^{1}H NMR (500 MHz, CD_2Cl_2) δ 7.72 (d, 1 H, J = 10.0 Hz), 7.52 (s, 1 H), 7.41 (d, 1 H, J = 3.5 Hz), 7.35−7.24 (m, 2 H), 7.13 (d, 1 H, J = 3.5 Hz), 6.89 (d, 1 H, J = 9.0 Hz), 3.72 (t, 4 H, J = 5.0 Hz), 3.60 (t, 2 H, J = 5.0 Hz), 3.29 (s, 3 H), 3.25 (s, 6 H), 1.82−1.72 (m, 4 H), 1.71−1.64 (m, 4 H), 1.14 (s, 6 H); ^{13}C NMR (300 MHz, $CDCl_3$) δ 162.1, 152.5, 151.1, 150.2, 145.1, 144.7, 140.4, 139.4, 137.3, 135.0, 131.6, 129.8, 128.2, 120.7, 120.0, 114.8, 108.7, 108.3, 48.5, 40.6, 40.2, 34.2, 31.8, 28.5, 26.1, 24.5; IR (film on NaCl) 2936, 2859, 1592, 1536, 1508, 1473, 1446, 1408, 1387, 1329, 1255, 1214 cm^{-1}; λ_{max} (MeOH) 609 nm (ε = 7.44 × 10^4 M^{-1} cm^{-1}); HRMS (ESI, HRDFMagSec) m/z 578.1739 (calcd for $C_{31}H_{36}N_3OS^{80}Se^+$, 578.1739). Anal. Calcd for $C_{31}H_{36}N_3OSSeCl\cdot3.25H_2O$: C, 55.44; H, 6.38; N, 6.26. Found: C, 55.20; H, 6.11; N, 6.18.

Determination of *n*-Octanol/Water Partition Coefficients. The octanol/water partition coefficients were all measured at pH 7.4 (PBS) at 23 °C using UV−visible spectrophotometry. The measurements were done using a shake flask direct measurement.[40] Mixing for 3−5 min was followed by 1 h of settling time. Liquid chromatography grade 1-octanol was used.

Determination of Singlet Oxygen Yields from Singlet Oxygen Luminescence Spectroscopy. Generation of $^1O_2$ was assessed at 1270 nm where its luminescence peaked. A spectrometer equipped with a NIR photodetector was used for acquisition of the emission spectra in NIR spectral range. A diode-pumped solid-state laser at 532 nm was the excitation source. The emission signal was collected at 90° relative to the exciting laser beam with the use of a 950 nm long-pass filter to attenuate the scattered light and fluorescence from the samples. A second harmonic (532 nm) from the nanosecond-pulsed Nd:YAG laser operating at 20 Hz was used as the excitation source for time-resolved measurements. The samples (CH_3OH solutions of the compounds in quartz cuvettes) were placed in front of the spectrometer entrance slit.

Fluorescence Experiments. Measurements of fluorescence quantum yield were performed on a spectrofluorometer using fluorescent dye **3** with known Φ_{FL} = 0.93 [38] in CH_3OH as standard.

Phototoxicity and Dark Toxicity Studies with Colo-26 Cells. All cells were grown in RPMI 1640, 1× with L-glutamine medium. The medium was supplemented with 10% fetal bovine serum (FBS) and 1% penicillin−streptomycin. Cells were harvested, plated 10 000 to a well in a 96-well plate (0.32 cm^2 on a flat bottom plate), and incubated for 24 h. Dyes were added from stock solutions of known concentration. All plates were incubated 1 h in the dark after dye addition and then either kept in the dark or irradiated with a tunable dye laser at λ_{max} (±2 nm) at a fluence rate of 3.2 mW cm^{-2} to various light doses. New medium was added to each well before they were placed in the incubator (37 °C, 5% CO_2). After a 48 h incubation, a sulforhodamine B assay[41,42] was performed on the plates. The

dx.doi.org/10.1021/jm501259v | J. Med. Chem. 2014, 57, 8622−8634

absorbance of each well was read on an EL800 BioTek plate reader at 570 nm to give fraction cell viability after data manipulation.

Combination Therapy with PDT and Doxorubicin in Colo-26 Cells. Colo-26 cells were harvested and plated 10 000 to a well, in 90 μL of medium per well, in a 96-well plate, and incubated for 24 h. Doxorubicin solutions in RPMI 1640 medium were made from a 20 mM Dox stock solution. Selenorhodamine dye solutions were made in RPMI 1640 medium from ethanol stock solutions of known concentration. Each dye was combined with each Dox concentration. To the selenorhodamine only wells, 10 μL of the 10× selenorhodamine solution was added. To the remaining wells, 10 μL of the 10× Dox-only solution or 10 μL of the combined 10× selenorhodamine + Dox solution was added to achieve the desired concentrations. The plates were incubated in the dark for 1 h and were then irradiated with a tunable dye laser at λ_{max} (±2 nm) at a fluence rate of 3.2 mW cm^{-2} to a light dose of 1 J cm^{-2}. The medium was flicked from the plates, and 100 μL of fresh medium was added to each well before they were placed in the incubator (37 °C, 5% CO_2). After a 48 h incubation, a sulforhodamine B assay[42,43] was performed on the plates. The absorbance of each well was read on an EL800 BioTek plate reader at 570 nm to give fraction cell viability after data manipulation.

Flow Cytometry Studies. Colo-26 cells were harvested, and flow cytometry was run on an LSR II A UV-Normal Flow instrument with an excitation wavelength of 561 nm (50 mW cm^{-2}) and an emission of 710 nm (50 PE-Cy 5.5). Image flow cytometry was run on an ImageStream Mark II instrument. The channels used were channels 2 (480−560 nm detection) and 5 (642−745 nm detection) with MTG excitation at 488 nm and selenorhodamine excitation at 561 nm. Samples were made using 5×10^5 Colo-26 cells in 0.5 mL of medium. Each photosensitizer had a total of six samples: the photosensitizer alone at three different concentrations (0.1, 0.2, and 0.4 μM), the photosensitizer at three different concentrations plus Mito-Tracker Green (MTG, 0.5 μL of 1 mM MTG stock in DMSO), and MTG alone (0.5 μL of 1 mM MTG stock in DMSO). All samples were incubated 15 min, centrifuged, and flicked. Hanks PBS (60 μL) was added to each sample to replace the medium. The samples were resuspended, put on ice, and analyzed. Colocalization was determined in each individual cell using the IDEAS similarity feature, which is a log-transformed Pearson's correlation coefficient of the intensities of the spatially correlated pixels within the whole cell, of the MTG and **15b−18b** images, MTG and Mito-Tracker Red (MTR) images, or LysoTracker Green (LYS) and MTR images, respectively. The similarity score is a measure of the degree to which two images are linearly correlated.[46]

Pgp-Transport Studies across MDCK-MDR1 Monolayers. MDCK-MDR1 cells were seeded at 50 000 cells cm^{-2} onto 12-well (1.13 cm^2 surface area) Transwell polycarbonate filters (Costar), were fed on days 3 and 5, and used on day 6. The upper and lower chamber volumes were 0.5 and 1.0 mL, respectively. Cells were rinsed 10 min in DPBSH at 37 °C with mixing on a nutator (Clay Adams). Cells were preincubated with 4.3 mg mL^{-1} bovine serum albumin (BSA) in DPBSH alone or containing 5 μM **24**. After 30 min, 5 μM test compound (**17b** or **18b**) in BSA/DPBSH with or without inhibitor was added to the donor chamber (0.5 mL upper or apical, 1.0 mL lower or basolateral). Initial donor samples were taken at $t = 0$. For apical-to-basolateral (AB) flux, D_0 was taken from the mixing tube before addition to the cell monolayer. For basolateral-to-apical (BA) flux this sample was taken from the 12-well plate 10 min after transfer but before cell wells were added. Samples were taken from both the donor and receiver chambers following a 1 h incubation at 37 °C with constant mixing by nutation. Cell monolayers were rinsed briefly two times using cold DPBS and extracted with 500 μL of CH_3OH for 3 min. In a 96-deep well assay plate, 50 μL samples were combined into $n = 3$ cassettes and protein was precipitated by adding 450 μL of CH_3CN and shaken to mix. Plates were centrifuged 5 min at 5000 rpm. Compound concentrations were determined with an LC−MS/MS assay. Chromatography was performed using a Betasil C18 2 mm × 20 mm, 5 μm Javelin column (Thermo Scientific, Waltham, MA) and one of two mobile phase systems. System 1 consisted of 5 mM ammonium bicarbonate in water (mobile phase A) and 5 mM NH_4HCO_3 in CH_3OH (mobile phase B), with elution accomplished by a CH_3OH gradient at 1.5 mL/min. System 2 consisted of 0.4% trifluoracetic acid (TFA), 1 mM NH_4HCO_3 in H_2O (mobile phase A), and 0.4% TFA/1 mM NH_4HCO_3 in CH_3CN (mobile phase B), with elution accomplished by an CH_3CN gradient at 1.5 mL/min. Mass spectrometric detection was performed with an API4000 mass spectrometer (Applied Biosystems, Foster City, CA) equipped with a turbo ion spray source, using selected reaction monitoring in positive ion mode with precursor and product ion transitions specific to each analyte.

Statistical Analyses. All statistical analyses were performed using the Student's *t*-test for pairwise comparisons. A p value of <0.05 was considered significant.

■ ASSOCIATED CONTENT

Ⓢ Supporting Information

Figures of electronic absorption spectra, singlet-oxygen decay traces, flow cytometry, dose−response curves for dark toxicity, with broadband light for **15a−18a**, with laser-irradiation for **15b−18b**, combination PDT and Dox treatment, and ImageStream flow cytometry showing mitochondrial localization. This material is available free of charge via the Internet at http://pubs.acs.org.

■ AUTHOR INFORMATION

Corresponding Author

*Phone: 716-645-4228. Fax: 716-645-6963. E-mail: mdetty@buffalo.edu.

Notes

The authors declare no competing financial interest.

[⊥]J.M.: Deceased June 5, 2014.

■ ACKNOWLEDGMENTS

We thank Dr. Piet Borst at The Netherlands Cancer Institute for supplying the MDCKII-MDR1 cells. This research was supported in part by the NIH Grant GM-94367 to M.R.D.

■ ABBREVIATIONS USED

ABC, ATP-binding cassette; BSA, bovine serum albumin; DLC, delocalized lipophilic cation; DMSO, dimethylsulfoxide; Dox, doxorubicin; DPBSH, Dulbecco's HEPES-containing phosphate buffered saline; FBS, fetal bovine serum; LDA, lithium diisopropylamide; LYS, 3-(5,5-difluoro-7,9-dimethyl-5*H*-4λ^4,5λ^4-dipyrrolo[1,2-*c*:2′,1′-*f*][1,3,2]diazaborinin-3-yl)-*N*-(2-(dimethylamino)ethyl)propanamide; MDCK, Madin−Darby canine kidney; MDR, multidrug resistant; MRP, multidrug resistance protein; MTG, 2-[3-[5,6-dichloro-1,3-bis[[4-(chloromethyl)phenyl]methyl]-1,3-dihydro-2*H*-benzimidazol-2-ylidene]-1-propenyl]-3-methylbenzoxazolium chloride; MTR, 9-[4-(chloromethyl)phenyl]-2,3,6,7,12,13,16,17-octahydro-[1*H*,5*H*,11*H*,15*H*]xantheno[2,3,4-*ij*:5,6,7-*i*′*j*′]diquinolizin-18-ium chloride; NIR, near-infrared; PDT, photodynamic therapy; P-gp, P-glycoprotein; PBS, phosphate buffered saline; THF, tetrahydrofuran; VER, verapamil; VIN, vinblastine

■ REFERENCES

(1) Gottesman, M. M.; Fojo, T.; Bates, S. E. Multidrug resistance in cancer: role of ATP-dependent transporters. *Nat. Rev. Cancer* **2002**, *2*, 48−58.

(2) Szakacs, G.; Paterson, J. K.; Ludwig, J. A.; Booth-Genthe, C.; Gottesman, M. M. Targeting multidrug resistance in cancer. *Nat. Rev. Drug Discovery* **2006**, *5*, 219−234.

(3) Abolhoda, A.; Wilson, A. I.; Ross, H.; Danenberg, P. V.; Burt, M.; Scotto, K. W. Rapid activiation of MDR1 gene expression in human

metastatic sarcoma after in vivo exposure to doxorubicin. *Clin. Cancer Res.* **1999**, *5*, 3352−3356.
(4) Raub, T. J. P-Glycoprotein recognition of substrates and circumvention through rational drug design. *Mol. Pharmaceutics* **2006**, *3*, 3−25.
(5) Seelig, A.; Gatlik-Landwojtowicz, E. Inhibitors of multidrug efflux transporters: their membrane and protein interactions. *Mini-Rev. Med. Chem.* **2005**, *5*, 135−151.
(6) Dantzig, A. H.; de Alwis, D. P.; Burgess, M. Considerations in the design and development of transport inhibitors as adjuncts to drug therapy. *Adv. Drug Delivery Rev.* **2003**, *55*, 133−150.
(7) Loetchutinat, C.; Saengkhae, C.; Marbeuf-Gueye, C.; Garnier-Suillerot, A. New insights into the P-glycoprotein-mediated effluxes of rhodamines. *Eur. J. Biochem.* **2003**, *270*, 476−485.
(8) Eytan, G. D.; Regev, R.; Hurwitz, C. D.; Assaraf, Y. G. Efficiency of P-glycoprotein-mediated exclusion of rhodamine dyes from multidrug-resistant cells is determined by their passive transmembrane movement rate. *Eur. J. Biochem.* **1997**, *248*, 104−112.
(9) Lu, P.; Liu, R.; Sharom, F. J. Drug transport by reconstituted P-glycoprotein in proteoliposomes. Effect of substrates and modulators, and dependence on bilayer phase state. *Eur. J. Biochem.* **2001**, *268*, 1687−1695.
(10) Johnson, L. V.; Walsh, M. L.; Bockus, B. J.; Chen, L. B. Monitoring of relative mitochondrial membrane potential in living cells by fluorescence microscopy. *J. Cell Biol.* **1981**, *88*, 526−535.
(11) Davis, S.; Weiss, M. J.; Wong, J. R.; Lampidis, T. J.; Chen, L. B. Mitochondrial and plasma membrane potentials cause unusual accumulation and retention of rhodamine 123 by breast adenocarcinoma-derived MCF-7 cells. *J. Biol. Chem.* **1985**, *260*, 13844−13850.
(12) Lampidis, T. J.; Bernal, S. D.; Summerhayes, I. C.; Chen, L. B. Selective toxicity of rhodamine-123 in carcinoma cells in vitro. *Cancer Res.* **1983**, *43*, 716−720.
(13) Bernal, S. D.; Lampidis, T. J.; McIsaac, R. M.; Chen, L. B. Anticarcinoma activity in vivo of rhodamine 123, a mitochondrial-specific dye. *Science* **1986**, *222*, 169−172.
(14) Sun, X.; Wong, J. R.; Song, K.; Hu, J.; Garlid, K. D.; Chen, L. B. AA1, a newly synthesized monovalent lipophilic cation, expresses potent in vivo antitumor activity. *Cancer Res.* **1994**, *54*, 1465−1471.
(15) Detty, M. R.; Gibson, S. L.; Wagner, S. J. Current clinical and preclinical photosensitizers for use in photodynamic therapy. *J. Med. Chem.* **2004**, *47*, 3987−3915.
(16) Pal, P.; Zeng, H.; Durocher, G.; Girard, D.; Li, T. C.; Gupta, A. K.; Giasson, R.; Blanchard, L.; Gaboury, L.; Balassy, A.; Turmel, C.; Laperriere, A.; Villeneuve, L. Phototoxicity of some bromine-substituted rhodamine dyes: synthesis, photophysical properties and application as photosensitizers. *Photochem. Photobiol.* **1996**, *63*, 161−168.
(17) Ohulchanskyy, T.; Donnelly, D. J.; Detty, M. R.; Prasad, P. N. Heteroatom substitution changes in excited-state photophysics and singlet oxygen generation in chalcogenoxanthylium dyes: effect of sulfur and selenium substitutions. *J. Phys. Chem. B* **2004**, *108*, 8668−8672.
(18) (a) Kessel, D.; Woodburn, K. Selective photodynamic inactivation of a multidrug transporter by a cationic photosensitizing agent. *Br. J. Cancer* **1995**, *71*, 306−310. (b) Ogata, M.; Inanami, O.; Nakajima, M.; Nakajima, T.; Hiraoka, W.; Kuwabara, M. Ca^{2+}-dependent and caspace-3-independent apoptosis caused by damage in Golgi apparatus due to 2,4,5,7-tetrabromorhodamine 123 bromide-induced photodynamic effects. *Photochem. Photobiol.* **2003**, *78*, 241−247.
(19) (a) Solomon, S. R.; Mielke, S.; Savani, B. N.; Montero, A.; Wisch, L.; Childs, R.; Hensel, N.; Schindler, J.; Ghetie, V.; Leitman, S. F.; Mai, T.; Carter, C. S.; Kurlander, R.; Read, E. J.; Vitetta, E. S.; Barrett, A. J. Selective depletion of alloreactive donor lymphocytes: a novel method to reduce the severity of graft-versus-host disease in older patients undergoing matched sibling donor stem cell transplantation. *Blood* **2005**, *106*, 1123−1129. (b) Mielke, S.; Nunes, R.; Rezvani, K.; Fellowes, V. S.; Venne, A.; Solomon, S. R.; Fan, Y.; Gostick, E.; Price, D. A.; Scotto, C.; Read, E. J.; Barrett, A. J. A clinical-scale selective allodepletion approach for the treatment of HLA-mismatched and matched donor-recipient pairs using expanded T lymphocytes as antigen-presenting cells and a TH9402-based photodepletion technique. *Blood* **2008**, *111*, 4392−4402.
(20) Detty, M. R.; Prasad, P. N.; Donnelly, D. J.; Ohulchanskyy, T.; Gibson, S. L.; Hilf, R. Synthesis, properties, and photodynamic properties in vitro of heavy-chalcogen analogues of tetramethylrosamine. *Bioorg. Med. Chem.* **2004**, *12*, 2537−2544.
(21) Scala, S.; Akhmed, N.; Rao, U. S.; Paull, K.; Lan, L.-B.; Dickstein, B.; Lee, J.-S.; Elgemeie, G. H.; Stein, W. D.; Bates, S. E. P-glycoprotein substrates and antagonists cluster into two distinct groups. *Mol. Pharmacol.* **1997**, *51*, 1024−1033.
(22) Lee, J. S.; Paull, K.; Alvarez, M.; Hose, C.; Monks, A.; Grever, M.; Fojo, A. T.; Bates, S. E. Rhodamine efflux patterns predict P-glycoprotein substrates in the National Cancer Institute drug screen. *Mol. Pharmacol.* **1994**, *46*, 627−638.
(23) Shapiro, A. B.; Ling, V. Stoichiometry of rhodamine 123 transport to ATP hydrolysis by P-glycoprotein. *Eur. J. Biochem.* **1998**, *254*, 189−193.
(24) Shapiro, A. B.; Ling, V. Positively cooperative sites for drug transport by P-glycoprotein with distinct drug specificities. *Eur. J. Biochem.* **1997**, *250*, 130−137.
(25) Tombline, G.; Donnelly, D. J.; Holt, J. J.; You, Y.; Ye, M.; Gannon, M. K.; Nygren, C. L.; Detty, M. R. Stimulation of P-glycoprotein ATPase by analogues of tetramethylrosamine: coupling of drug binding at the "R" site to the ATP hydrolysis transition state. *Biochemistry* **2006**, *45*, 8034−8047.
(26) Tombline, G.; Holt, J. J.; Gannon, M. K., II; Donnelly, D. J.; Wetzel, B.; Sawada, G. A.; Raub, T. J.; Detty, M. R. ATP occlusion as a surrogate measure for drug coupling. *Biochemistry* **2008**, *47*, 3294−3307.
(27) Gannon, M. K., II; Holt, J. J.; Bennett, S. M.; Wetzel, B. R.; Loo, T. W.; Bartlett, M. C.; Clarke, D. M.; Sawada, G. A.; Higgins, J. W.; Tombline, G.; Raub, T. J.; Detty, M. R. Rhodamine inhibitors of P-glycoprotein: an amide/thioamide "switch" for ATPase activity. *J. Med. Chem.* **2009**, *52*, 3328−3341.
(28) Orchard, A.; Schamerhorn, G. A.; Calitree, B. D.; Sawada, G. A.; Loo, T. W.; Bartlett, M. C.; Clarke, D. M.; Detty, M. R. Thiorhodamines containing amide and thioamide functionality as inhibitors of the ATP-binding cassette drug transporter P-glycoprotein (*ABCB1*). *Bioorg. Med. Chem.* **2012**, *20*, 4290−4302.
(29) Gorman, A.; Killoran, J.; O'Shea, C.; Kenna, T.; Gallagher, W. M.; O'Shea, D. F. In vitro demonstration of the heavy-atom effect for photodynamic therapy. *J. Am. Chem. Soc.* **2004**, *126*, 10619−10631.
(30) Leonard, K. A.; Hall, J. P.; Nelen, M. I.; Davies, S. R.; Gollnick, S. O.; Camacho, S.; Oseroff, A. R.; Gibson, S. L.; Hilf, R.; Detty, M. R. A selenopyrylium photosensitizer for photodynamic therapy related in structure to the antitumor agent AA1 with potent in vivo activity and no long-term skin photosensitization. *J. Med. Chem.* **2000**, *43*, 4488−4498.
(31) Brennan, N. K.; Hall, J. P.; Davies, S. R.; Gollnick, S. O.; Oseroff, A. R.; Gibson, S. L.; Hilf, R.; Detty, M. R. In vitro photodynamic properties of chalcogenopyrylium analogues of the thiopyrylium antitumor agent AA1. *J. Med. Chem.* **2002**, *45*, 5123−5135.
(32) Detty, M. R.; Gibson, S. L.; Hilf, R. Comparison of the dark and light-induced toxicity of thio and seleno analogues of the thiopyrylium dye AA1. *Bioorg. Med. Chem.* **2004**, *12*, 2589−2596.
(33) Holt, J. J.; Gannon, M. K.; Tombline, G.; McCarty, T. A.; Page, P. M.; Bright, F. V.; Detty, M. R. A cationic chalcogenoxanthylium photosensitizer effective in vitro in chemosensitive and multidrug-resistant cells. *Biorg. Med. Chem.* **2006**, *14*, 8635−8643.
(34) Kryman, M. W.; Schamerhorn, G. A.; Hill, J. E.; Calitree, B. D.; Davies, K. S.; Linder, M. K.; Ohulchanskyy, T. Y.; Detty, M. R. Synthesis and properties of heavy chalcogen analogues of the Texas reds and related rhodamines. *Organometallics* **2014**, *33*, 2628−2640.
(35) Beak, P.; Brown, R. A. The tertiary amide as an effective director of ortho lithiation. *J. Org. Chem.* **1982**, *47*, 34−36.

(36) Carpenter, A. J.; Chadwick, D. J. High yield syntheses of 2,3-disubstituted furans and thiophenes. *Tetrahedron Lett.* **1985**, *26*, 1777−1980.
(37) Katritzky, A. R.; Witek, R. M.; Rodriguez-Garcia, V.; Mohapatra, P. P.; Rogers, J. W.; Cusido, J.; Abdel-Fattah, A. A. A.; Steel, P. J. Benzotriazole-assisted thioacylation. *J. Org. Chem.* **2005**, *70*, 7866−7881.
(38) Magde, D. R.; Wong, R.; Seybold, P. G. Fluorescence quantum yields and their relation to lifetimes of rhodamine 6G and fluorescein in nine solvents: improved absolute standards for quantum yields. *Photochem. Photobiol.* **2002**, *75*, 327−334.
(39) Partition Coefficients: Sangster, J. In *Octanol−Water Partition Coefficients: Fundamentals and Physical Chemistry*; Fogg, P. G. T., Ed.; Wiley Series in Solution Chemistry, Vol. 2; John Wiley and Sons: New York, 1997.
(40) Spoelstra, E. C.; Dekker, H.; Schuurhuis, G. J.; Broxterman, H. J.; Lankelma, J. P-glycoprotein drug efflux pump involved in the mechanisms of intrinsic drug resistance in various colon cancer cell lines. Evidence for a saturation of active daunorubicin transport. *Biochem. Pharmacol.* **1991**, *41*, 349−359.
(41) Evers, R.; Kool, M.; Smith, A. J.; van Deemter, L.; de Haas, M.; Borst, P. Inhibitory effect of the reversal agents V-104, GF120918 and Pluronic L61 on MDR1Pgp-, MRP1- and MRP2-mediated transport. *Br. J. Cancer* **2000**, *83*, 366−374.
(42) Houghton, P.; Fang, R.; Techatanawat, I.; Steventon, G.; Hylands, P. J.; Lee, C. C. The sulphorhodamine (SRB) assay and other approaches to testing plant extracts and derived compounds for activities related to reputed anticancer activity. *Methods* **2007**, *42*, 377−387.
(43) Vichai, V.; Kirtikara, K. Sulforhodamine B colorimetric assay for cytotoxicity screening. *Nat. Protoc.* **2006**, *1*, 1112−1116.
(44) Sawada, G. A.; Barsuhn, C. L.; Lutzke, B. S.; Houghton, M. E.; Padbury, G. E.; Ho, N. F. H.; Raub, T. J. Increased lipophilicity and subsequent cell partitioning decrease passive transcellular diffusion of novel, highly lipophilic antioxidants. *J. Pharmacol. Exp. Ther.* **1999**, *288*, 1317−1326.
(45) Dantzig, A. H.; Shepard, R. L.; Law, K. L.; Tabas, L.; Pratt, S.; Gillespie, J. S.; Binkley, S. N.; Kuhfeld, M. T.; Starling, J. J.; Wrighton, S. A. Selectivity of the multidrug resistance modulator, LY335979, for P-glycoprotein and effect on cytochrome P450 activities. *J. Pharmacol. Exp. Ther.* **1999**, *290*, 854−890.
(46) Riddell, J. R.; Wang, X.-Y.; Hans Minderman, H.; Gollnick, S. O. Peroxiredoxin 1 stimulates secretion of proinflammatory cytokines by binding to TLR4. *J. Immunol.* **2010**, *184*, 1022−1030.
(47) Wagner, S. J.; Skripchenko, A.; Donnelly, D. J.; Ramaswamy, K.; Detty, M. R. Chalcogenoxanthylium photosensitizers for the photodynamic purging of blood-borne viral and bacterial pathogens. *Bioorg. Med. Chem.* **2005**, *13*, 5927−5935.
(48) Wagner, S. J.; Skripchenko, A.; Thompson-Montgomery, D.; Awatefe, H.; Donnelly, D. J.; Detty, M. R. Use of a red cell band 3-ligand/antioxidant to improve red cell storage properties following virucidal phototreatment with chalcogenoxanthylium photosensitizers for pathogen reduction. *Photochem. Photobiol.* **2006**, *76*, 514−517.
(49) Calitree, B. D.; Donnelly, D. J.; Holt, J. J.; Gannon, M. K., II; Nygren, C.; Sukumaran, D. K.; Autschbach, J.; Detty, M. R. Tellurium analogues of rosamine and rhodamine dyes: synthesis, structure, ^{125}Te NMR, and heteroatom contributions to excitation energies. *Organometallics* **2007**, *26*, 6248−6257.
(50) Weiss, R. B. The anthracyclines: Will we ever find a better doxorubicin? *Semin. Oncol.* **1992**, *19*, 670−686.
(51) Jordon, M. A. Anti-cancer agents. *Cur. Med. Chem.* **2002**, *2*, 1−17.
(52) Chatterjee, K.; Zhang, J.; Honbo, N.; Karliner, J. S. Doxorubicin cardiomyopathy. *Cardiology* **2010**, *115*, 155−162.